NANO LETTERS

pubs.acs.org/NanoLett

Radiative Heat Pumping from the Earth Using Surface Phonon Resonant Nanoparticles

A. R. Gentle,* and G. B. Smith*

Department of Physics and Advanced Materials, University of Technology, Sydney, P.O. Box 123, Broadway, NSW, 2007 Australia

ABSTRACT Nanoparticles that have narrow absorption bands that lie entirely within the atmosphere's transparent window from 7.9 to 13 μm can be used to radiatively cool to temperatures that are well below ambient. Heating from incoming atmospheric radiation in the remainder of the Planck radiation spectrum, where the atmosphere is nearly "black", is reduced if the particles are dopants in infrared transmitting polymers, or in transmitting coatings on low emittance substrates. Crystalline SiC nanoparticles stand out with a surface phonon resonance from 10.5 to 13 μm clear of the atmospheric ozone band. Resonant SiO_2 nanoparticles are complementary, absorbing from 8 to 10 μm, which includes atmospheric ozone emissions. Their spectral location has made SiC nanoparticles in space dust a feature in ground-based IR astronomy. Optical properties are presented and subambient cooling performance analyzed for doped polyethylene on aluminum. A mixture of SiC and SiO_2 nanoparticles yields high performance cooling at low cost within a practical cooling rig.

KEYWORDS Surface phonon resonance, radiative sky cooling, SiC nanoparticles, SiO_2 nanoparticles, spectral selective emittance

Net radiant heat loss to the sky from surfaces whose temperature T_s is below ambient is not possible or weak within the Planck radiation spectrum at wavelengths λ where the atmosphere is opaque or has low transmittance. Conversely most radiant heating of surfaces under a clear sky at night is due to incoming radiation from these opaque bands. Thus surfaces that have very limited absorption in the opaque band, but absorb strongly in the transparent "sky window" between 7.9 to 13 μm, can cool to temperatures substantially below ambient if nonradiative heat gains across the temperature difference $[T_a - T_s]$ are kept small. T_a is the ambient temperature. Surfaces with spectral emittance, $e(\lambda) = 1.0$ for 7.9 μm $< \lambda <$ 13 μm, and $e(\lambda) = 0$ for 2 μm $< \lambda <$ 7.9 and 32 μm $> \lambda >$ 13 μm, are thus ideal limits for this function. These λ ranges are for Planck radiation spectra $P(\lambda,T_a)$ with T_a ranging from ambient to 20 °C below ambient. The sky window, even for clear conditions, is not totally free of absorption, and the residual absorption bands will be shown to play a key role in the optimum nanoparticles for cooling to the full sky hemisphere.

The sharp spectral tuning supplied by select phonon resonant nanoparticles, when used as dopants in infrared (IR) transparent polymers, or within suitable thin films on IR reflecting substrates, enables composite material absorption spectra which lie almost entirely within the sky window. This feature means it is then practical by adjusting the nanoparticle concentration to emit strongly within the sky window while transmitting or reflecting with weak absorption where the atmosphere is opaque.

* To whom correspondence should be addressed. E-mail: (G.B.S.) g.smith@uts.edu.au; (A.R.G.) angus.gentle@uts.edu.au.

Received for review: 07/17/2009
Published on Web: 01/07/2010

Radiative cooling has two components, thermal emission to the full sky hemisphere, and absorption of radiation emitted by the atmosphere. A complete description of the radiative cooling capabilities of a material thus requires knowledge of it is direction dependent surface spectral absorptance $a_s(\lambda,\eta)$, where η is the angle of incidence. Material absorptance $a_s(\lambda,\eta)$ governs the directional dependence of emitted radiation since $a_s(\lambda,\eta) = e_s(\lambda,\eta)$. It also determines absorptance of incoming radiation from the atmosphere at angle of incidence η. If the surface of interest is horizontal angle η also defines the angle to the zenith (or the vertical) at which atmospheric radiation is emitted. The intensity of this incoming radiation is determined by the atmosphere's direction dependent spectral emittance $e_a(\lambda,\eta) = a_a(\lambda,\eta) = [1 - t_a(\lambda,\eta)]$ with $a_a(\lambda,\eta)$ absorptance and $t_a(\lambda,\eta)$ the direction dependent transmittance of the atmosphere. An approximate "box" model of $e_a(\lambda,\eta)$ for a U.S. standard atmosphere has been used for indicative estimates of the cooling performance of sky window spectral selective materials in past studies.[1] Because this approximation assumes independence of λ from 7.9 to 13 μm it does not discriminate between the finer spectral responses of different phonon resonant nanoparticles inside the sky window. The value of this capability follows from a detailed analysis of the normal incidence atmospheric spectral transmittance $t_a(\lambda,0)$ for clear dry conditions, appearing in Figure 1. The broad goal is usually taken to be a material with high absorptance between the vertical bars in Figure 1 and very low absorptance outside this zone. We will demonstrate that a mix of two resonant nanoparticles, SiO_2 and SiC, can be used to get close to this ideal. However absorptance tuning to avoid the prominent ozone peak has added

DOI: 10.1021/nl903271d | *Nano Lett.* **2010,** *10,* 373-379

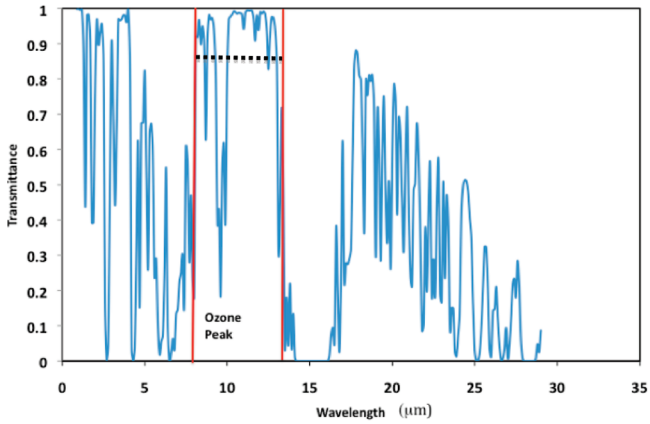

FIGURE 1. Atmospheric transmittance $t_a(\lambda,0) = 1 - e_a(\lambda,0)$, for a clear, very dry atmosphere (water vapor pressure 1.83 mm). The sky window range is outlined with two vertical lines and the horizontal dashed line is the "box model" approximation[1] to the average sky window transmittance at $\eta = 0°$.

benefits. Other weaker bands in this range are due to CO_2 and H_2O. SiC resonant nanoparticles are so finely tuned that they avoid absorbing the radiation coming in from the prominent ozone band in Figure 1, while still emitting only inside the sky window. The gains in doing this can be very significant at temperatures well below ambient and are magnified as η increases from the zenith, when all emission bands strengthen exponentially with atmospheric thickness. Thus for the nanomaterials in this study a box model of the sky window does not highlight the relative merits of SiC. Precise atmospheric models are thus used in our models of cooling performance.

Cooling performance is also very sensitive to local humidity levels. As they increase absorption in the sky window increases, so much higher net output and colder temperatures are possible under clear skies in Arizona compared to Florida, or Alice Springs than Sydney. To model material performance under a particular sky we first set humidity, then model $t_a(\lambda,0)$ for the gas mix of interest. In the "box" approximation to the US Standard clear atmosphere[1] $t_a(\lambda,0)$ has a constant value of 0.87 across the sky window as drawn in Figure 1. For simplicity and for easier comparison to these prior material studies, we confine to the atmosphere used in Figure 1, as that gives an average value across the "sky window" that matches the "box" model value. $e_a(\lambda,\eta)$ is then found from $t_a(\lambda,0)$ using eq 1, where the factor $1/\cos\eta$ arises from the thickness $d_a(\eta)$ of the atmosphere at angle η to the zenith since $d_a(\eta) = d_a(0)/\cos\eta$,

$$e_a(\lambda,\eta) = 1 - [t(\lambda,0)]^{1/\cos\eta} \qquad (1)$$

For a surface at temperature T_s open to the sky the net cooling power is given by eq 2

$$P_{rad} = \left[\int_0^{\pi/2} d(\sin^2\eta) \int_0^{\infty} d\lambda\, P(\lambda, T_s) e_s(\eta,\lambda)\right] - \left[\int_0^{\pi/2} d(\sin^2\eta) \int_0^{\infty} d\lambda\, P(\lambda, T_a) e_a(\eta,\lambda) e_s(\eta,\lambda)\right] \qquad (2)$$

The first term is the outgoing power, the second term is the incoming atmospheric radiation from the full sky hemisphere that is absorbed. The smaller this second term becomes, the lower T_s can fall below ambient before $P_{rad} = 0$. This last condition defines the radiation stagnation temperature and with phonon resonant nanoparticles we shall show it can be 35−50 °C below ambient. If integration over η is done first the two remaining integrand terms from eq 2 are spectral power densities. These two spectra are of considerable value when linking materials design to operating cold temperature range and local atmospheric conditions. They also provide visual insight into the origins of the cooling benefits of each resonant nanoparticle. Examples follow.

Practical radiative cooling may involve cooling objects, or spaces to as low a temperature as possible, or pumping heat at useful rates from a fluid at a temperature that is cold, but well above stagnation. Equation 2 has to be modified if useful heat pumping rates are needed at temperatures 5 °C or more below ambient. Then it is important to limit non-radiative heat gains, which rise in proportion to $(T_a - T_s)$. Doing so impacts on radiation exchange in various ways. To reduce convective gains due to warmer local air and local air-flow, an IR transmitting polymer cover is typically placed a few centimeters above the cooling surface. Incidental benefits of this cover are to keep dust off the radiating surface and to limit the amount of water that condenses. A little dust on the cover is found to have little or no impact on performance, as it typically contains compounds that radiate well. Excessive dirt would need to be cleaned off if there was no rain, as is also done for solar technologies. Moderate condensation on the radiating surface is not a problem, though some cooling power sometimes goes into freezing such water droplets. Surfaces like those we discuss in this paper can achieve 15 °C below the coldest ambient of the night when covers are present with 8 mm water vapor pressure. Thus freezing water drops do occur.

The impact of the cover on the terms in eq 2 is as follows. The power leaving the surface is not affected as it depends only on T_s. To find the incoming power density before absorption, $P(\lambda,T_a)e_a(\lambda,\eta)$ is replaced by three terms, (i) $t_c(\eta,\lambda)P(\lambda,T_a)e_a(\eta,\lambda)$, (ii) $r_c(\eta,\lambda)P(\lambda,T_s)e_s(\eta,\lambda)$, and (iii) $e_c(\eta,\lambda)P(\lambda,T_a)$, to yield eq 3. The coefficients $t_c(\lambda,\eta)$ and $r_c(\lambda,\eta)$ are respectively the directional dependent spectral transmittance and reflectance of the cover, and $e_c(\lambda,\eta) = 1 - t_c(\lambda,\eta) - r_c(\lambda,\eta)$, is the relevant emittance of the cover. These three quantities are easily found either directly from data on the cover sheet, or from the optical constants and thickness of the polymers used. Term (i) amounts to a reduction in the incoming radiation due to the cover, while terms (ii) and (iii) add to it. Term (iii) is the contribution of

DOI: 10.1021/nl903271d | *Nano Lett.* **2010,** *10,* 373-379

thermal emission from the cover. The polymer is always in practice at a temperature very close to ambient temperature T_a so we can assume that any slight tendency it has to warm due to weak absorption of radiation emitted from the surface of interest can be neglected

$$P_{rad} = \left[\int_0^{\pi/2} d(\sin^2\eta) \int_0^{\infty} d\lambda\, P(\lambda, T_s) e_s(\eta, \lambda)\right] - \left\{\int_0^{\pi/2} d(\sin^2\eta) \int_0^{\infty} d\lambda\, e_s(\eta, \lambda)[P(\lambda, T_a) t_c(\eta, \lambda) e_a(\eta, \lambda) + P(\lambda, T_s) r_c(\eta, \lambda) e_s(\eta, \lambda) + P(\lambda, T_a) e_c(\eta, \lambda)]\right\} \quad (3)$$

A variety of single layer coatings such as MgO, SiO, SiO_2, and SiO_xN_{1-x} on low emittance metal substrates have been considered for this task.[2−5] They must be at least a micrometer thick for peak absorption close to 100%. No single material fills the desired absorption band completely and significant spillover of absorption outside the sky window can occur. Secondary absorption peaks where reflection is desired should be avoided but arise with some of these materials. Nanoparticles with suitable absorption bands do not seem to have been considered, but have a number of advantages in being suited to low cost large area composites in various formats. They can supply the desired absorption in coatings on low e substrates, but also can be embedded within polymer foils or thin sheets which are IR transmitting to achieve the desired absorption profile. Nanoparticles are easily embedded within the polymer material when it is formed. Microparticles of the materials listed above might be considered for this task. However while providing useful absorption they may also backscatter where absorption is strong, which reduces $e(\lambda)$. Backscattering is accentuated when multiple scattering occurs within microparticle composites, but with small enough nanoparticles and $\lambda > 7.9\,\mu$m it should not be a concern. Thus nanoparticles which resonate in the desired wavelength range are ideal for this cooling task.

The materials considered to date for spectral selective sky cooling rely on the normal bulk phonon modes in uniform coatings of low molecular weight compounds. This paper is about the potential for inorganic materials which cannot be used in single layer thin film form because in that form they reflect strongly between 7.9 to 13 μm. They reflect because within this band their dielectric constant ε, as given by eq 4, is negative between ω_L and ω_T. These are respectively the transverse and longitudinal optical phonon frequencies at zero phonon wave-vector and define the Reststrahlen band. $\varepsilon(0)$ is the static response and $\varepsilon(\infty)$ the residue from high frequency absorption. These Reststrahlen materials are analogous to plasmonic metal, which reflect as uniform layers but have sharp resonances as nanoparticles

$$\varepsilon(\omega) = \varepsilon(\infty) + \frac{\omega_T^2[(\varepsilon(0) - \varepsilon(\infty))]}{\omega_T^2 - \omega^2 - i\omega\omega_\tau} = \varepsilon(\infty)\left[1 + \frac{\omega_L^2 - \omega_T^2}{\omega_T^2 - \omega^2 - i\omega\omega_\tau}\right] \quad (4)$$

Relaxation frequency is ω_τ. Within the Reststrahlen band, one can excite surface phonons (SPh) on nanoparticles and surface phonon polaritons (SPhP) on smooth layers. These SPh resonances on small nanoparticles are well-known and are easily modeled from dipole polarizability.[6] The resonance peak occurs at $\omega = \omega_{res}$ as given by eq 5 for a sphere embedded in a medium with dielectric constant ε_h. If this resonance is almost completely localized within the sky window range the nanoparticle is an excellent candidate for radiative cooling

$$\omega_{res}^2 = \frac{\omega_T^2(2\varepsilon_h) + \omega_L^2\varepsilon(\infty)}{2\varepsilon_h + \varepsilon(\infty)} \quad (5)$$

Crystalline and partly crystalline SiO_2 and crystalline SiC have $\varepsilon < 0$ within the sky window zone in Figure 1. Both nanoparticles are thus of interest here. Other nanoparticles with ω_{res} in the right range are BN and BeO.[7] SiC is the standout nanoparticle for cooling because its nanosphere resonance is at a near ideal location peaking at 11.3 μm, since $\omega_L = 0.119$ eV (10.42 μm), $\omega_T = 0.098$ eV (12.6 μm), and $\varepsilon(0) = 9.72$, $\varepsilon(\infty) = 6.7$. The resonance is very sharp with $\omega_\tau(\mathrm{SiC}) = 0.0065$ eV. It is thus not only localized inside the sky window but also within its least absorbing section. In contrast $\omega_\tau(\mathbf{BN}) = 0.50$ eV, which is nearly 2 orders of magnitude larger, so its SPh resonance is too broad for the desired spectral selectivity. The absorption properties of SiC nanoparticles have been widely studied by astronomers[8,9] as they are pervasive in space dust, which leaves a sharp spectral signature within the IR radiation from deep space. The fact their narrow resonance lies entirely within the clearest part of the radiative window of earth's atmosphere has clearly aided ground-based IR astronomy, but its ability to efficiently send radiation away from earth does not seem to have been previously recognized. Hence the technological implications of SiC nanoparticles for low cost large area cooling have gone unnoticed.

Spectral reflectance $R(\lambda)$ of 25 μm thick doped polymer foils, both free-standing and attached to smooth aluminum sheet, were calculated using standard thin film models that require the complex optical constants $n(\omega) + ik(\omega) = \varepsilon(\omega)$ and foil thickness. We use thin film equations to model optical response at all angles of incidence since foil thickness is uniform and interference oscillations are seen in its optical response. That is, phase relations across the foil are pre-

DOI: 10.1021/nl903271d | Nano Lett. 2010, 10, 373-379

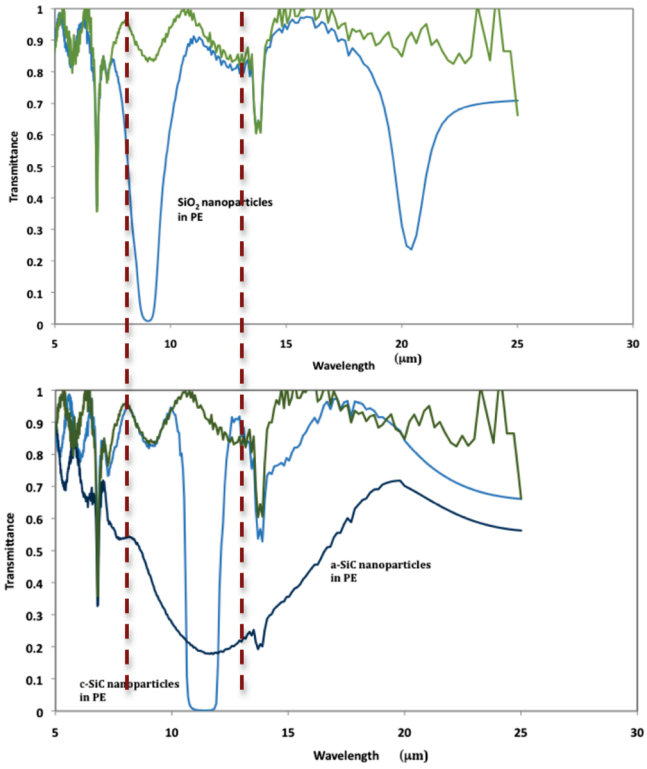

FIGURE 2. Two nanoparticle surface phonon resonant absorption bands peaking within the sky window (defined by the dashed lines). (Top) SiO_2 nanospheres; (Bottom) c-SiC and a-SiC nanospheres. All are embedded in 25 μm thick free-standing polyethylene. The a-SiC nanospheres are at twice the concentration of c-SiC and SiO_2. The undoped polyethylene foil data is also included.

served. The nanoparticles of interest are approximately 50 nm in diameter and spherical. Thus IR wavelengths in the Planck radiation range are on average around 200 times larger than particle size so scattering off each particle is negligible and quasi-static effective medium (EM) models can be used to find $\varepsilon(\omega)$ as a function of particle concentrations. In 25 μm thickness layers, nanoparticle concentrations of 10% for free-standing sheet and 5% if on aluminum give peak absorption approaching 100%. Maxwell Garnett[10] and Bruggeman[11] EM models give nearly identical answers for $\varepsilon(\omega)$ under these conditions. The $\varepsilon(\omega)$ used when the two nanoparticles SiC and SiO_2 are mixed into the polymer to absorb across the sky window were obtained by solving the EM eq 6, where f_c denotes the volume fraction of component c. The solution with just one of these nanoparticles present follows by dropping the appropriate one of the last two terms in eq 6

$$f_{PE}\frac{\varepsilon_{PE}-\varepsilon}{\varepsilon_{PE}+2\varepsilon}+f_{SiO_2}\frac{\varepsilon_{SiO_2}-\varepsilon}{\varepsilon_{SiO_2}+2\varepsilon}+f_{SiC}\frac{\varepsilon_{SiC}-\varepsilon}{\varepsilon_{SiC}+2\varepsilon}=0 \quad (6)$$

The PE optical data in Figure 2 was measured and PE optical constants were extracted from this undoped foil data

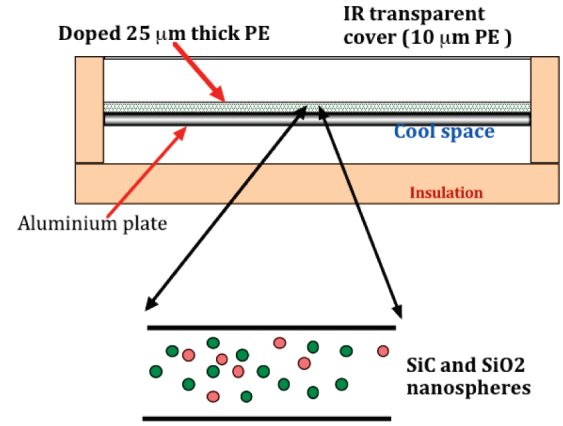

FIGURE 3. Schematic of a practical system modeled using eq 2 modified for the impact of the PE cover. This could be a small refrigerator or the low emittance metal plate could contain heat exchange channels for fluid cooling and be up against the base insulation.

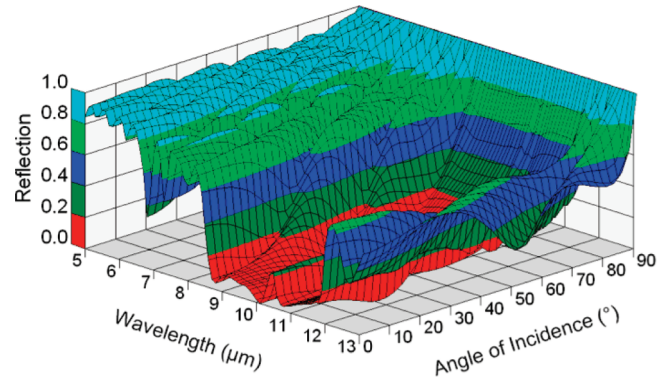

FIGURE 4. Reflectance as a function of wavelength and angle of incidence for doped polyethylene foil on aluminum. The foil contains a nanoparticle mix of 5% by volume of SiC and 5% by volume of SiO_2.

for use in eq 6. SiC and SiO_2 optical constant data is from Palik.[12] Modeled transmittance showing the resonant absorption of polytheylene foil doped with 10% c-SiC or SiO_2 nanospheres are compared at normal incidence in Figure 2 for free-standing foils. A distinguishing feature for the SiO_2 SPh resonance is it is straddling of the narrow ozone absorption/emission band centered at 9.7 μm in Figure 1. This has implications for sky cooling. Absorption with 20% amorphous SiC (a-SiC) nanoparticles, which do not support surface phonons, is also compared in Figure 2 to highlight the relative benefits of having $\varepsilon(\omega) < 0$.

The simplest complete cooling system to rigorously model based on eq 3 involves doped layers in contact with Al sheet under a PE cover as sketched in Figure 3. Spectral reflectance covering the full angle of incidence range must first be established. An example is in the three-dimensional plot of Figure 4 for a mixture of 5% SiC and 5% SiO_2 nanoparticles in 25 μm PE on aluminum. Reported systems testing of sky window spectral selective materials has been mainly confined to systems utilizing coated low emittance substrates in similar ar-

DOI: 10.1021/nl903271d | Nano Lett. 2010, 10, 373-379

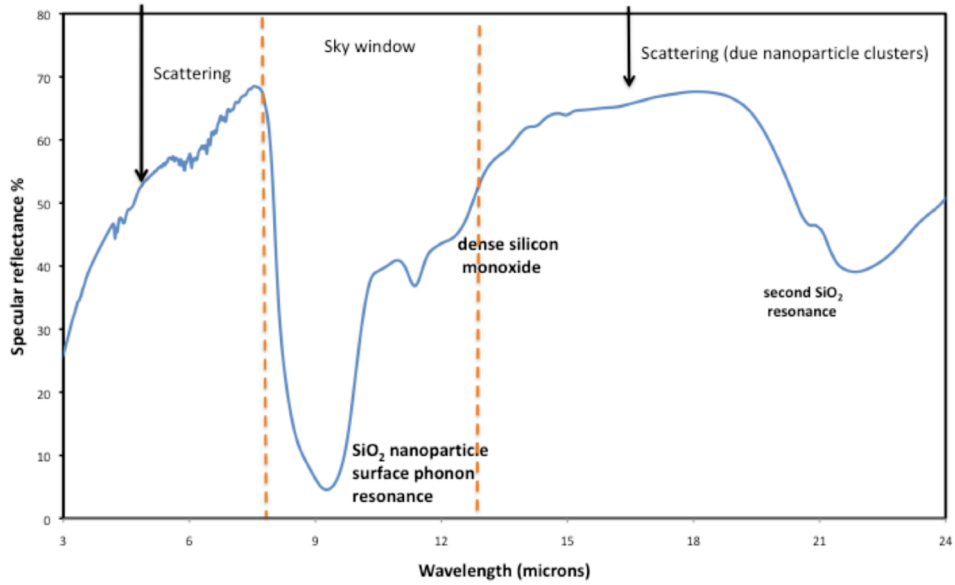

FIGURE 5. Measured specular reflectance across thermal radiation wavelengths for a nanocomposite film of SiO_2 nanoparticles overcoated with SiO.

rangements. IR spectral selectivity in free-standing polymers has applications potential but prior to this work suitable dopants had not been identified. Our results provide incentive to such studies in the future. The Al substrate introduces slightly more complex interference effects than in the free-standing foil of Figure 2, but the desired reflectance trough across the sky window is apparent to 70° incident angles in Figure 4. Additional absorption outside the sky window arises from a second resonant peak in SiO_2 nanoparticles near 20 μm, as in Figure 2, and from a combination of interference effects and intrinsic absorption peaks in the polyethylene which are amplified on Al relative to the free-standing case. The impact of these features on net cooling is weak except at very cold temperatures and are accounted for in the modeling of cooling powers below.

To verify the surface phonon resonance impact on a low e substrate, we spray-deposited SiO_2 nanoparticles onto an aluminum layer then overcoated them with SiO to form a nanocomposite. An example specular reflectance spectrum at normal incidence appears in Figure 5. The sharp absorption band is located where it is expected to be for SiO_2 nanoparticles embedded in SiO. These nanoparticles were clustered and the specular data in Figure 5 shows clear evidence of some resultant scattering. However it is primarily backscattering, so the emittance outside the sky window remains low as required. This was confirmed by the measured emittance of 0.41, which is close to what was aimed for in this film. Thus clustering does not appear to be a problem but can be avoided in the polymers. The deposited SiO was limited to a mass thickness of 260 nm to allow the particle resonance to stand-out. The performance of the simple experimental cooling system in Figure 3 was modeled using eq 2 for three different nanoparticle dopings, 5% SiC, 5% SiO_2, and 5% of each mixed together. The incoming and outgoing spectral power densities when the surface and the atmosphere are both at ambient with $T_a = T_s = 17$ °C, are plotted in Figure 6. Their difference yields after integration net radiant output. As the surface temperature T_s cools below ambient the outgoing density plot shrinks but for a fixed ambient the incoming/absorbed density plot does not change. The clear atmosphere in this plot is very dry, with 1.826 mm of water vapor pressure, $T_a = T_{\text{dry bulb}} = 17$ °C, $T_{\text{wet bulb}} = 6.5$ °C. This gave resulting average sky window transmittance near the zenith of 0.87, to match Figure 1. To find $e_a(\lambda,\eta)$, data was extracted using the program BTRAM, which is based on the 2004 version of HITRAN.[13] At this low humidity ozone is the main trace atmospheric emitter within the sky window and causes the large spike in the absorbed plot near 10 μm when SiO_2 nanoparticles are present. In contrast the c-SiC nanoparticle resonance is so narrow it does not absorb ozone emission but still lies completely within the sky window. Plots like Figure 6 provide relative performance insights for each material as the trace gas content in the atmosphere varies. Such information is very useful for composite materials optimization. As T_s drops it can be seen why c-SiC nanoparticles are so valuable for this technology. Their output curve has a long way to fall before its integrated output matches that for the absorbed term.

From these plots we expect stagnation when $P_{\text{rad}} = 0$ to occur at a lower temperature for SiC than either SiO_2 or the mixture of nanoparticles. Stagnation is dominated by how low the absorbed term goes, but keeping this low also reduces the output intensity. Thus the optimum material depends on the desired operating temperature relative to ambient. To complete this analysis and to see the changes that occur in the relative merits of each material as $(T_a - T_s)$ increases, Figure 7 plots the net output radiative power as a function of how cold T_s gets relative to ambient for the cooling system in Figure 3.

DOI: 10.1021/nl903271d | *Nano Lett.* **2010,** *10,* 373-379

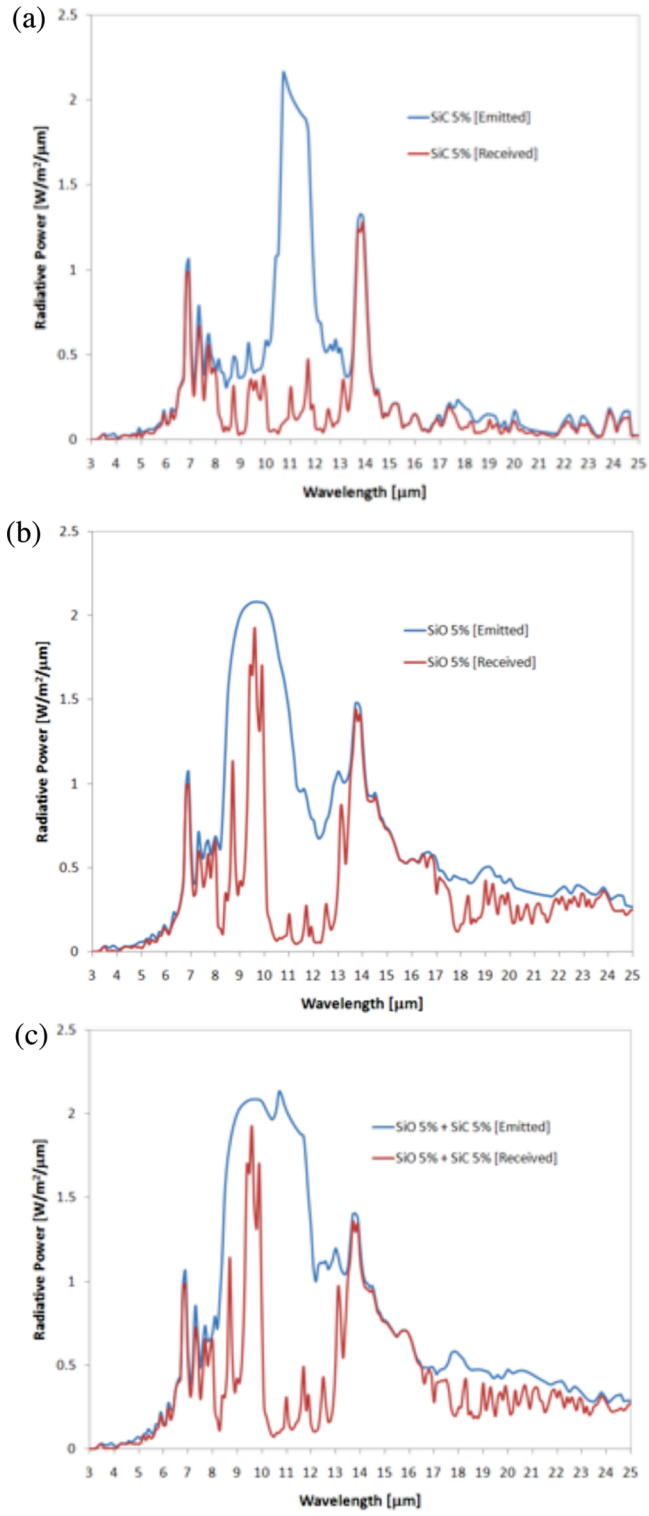

FIGURE 6. Emitted and absorbed spectral power densities for 25 μm thick doped PE on Al. Doping concentrations are (a) 5% by volume of c-SiC nanospheres (b) 5% by volume of SiO_2 nanospheres (c) the nanospheres in (a) and (b) combined. The large spike just below 10 μm in (b) and (c) is due to atmospheric ozone; the spike near 14 μm is due to the PE.

The sample with the mix of both nanoparticles gives superior cooling performance over most of the range but SiC

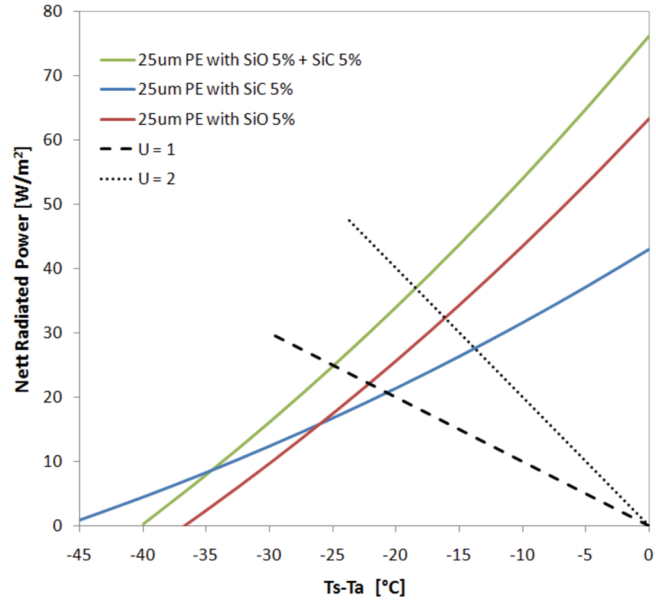

FIGURE 7. Net radiant output power as a function of ($T_s - T_a$) for the three nanoparticle doped 25 μm PE foils on aluminum of Figure 5 placed within the cooling set up in Figure 3. Ambient conditions are very dry as before with 1.826 mm of water vapor pressure. The rising heat input from convection and conduction as T_s drops is also shown for combined U values of 2 Wm^{-2} $°C^{-1}$ and 1 Wm^{-2} $°C^{-1}$.

nanoparticles by themselves are able to achieve the lowest radiative stagnation temperature because they absorb least. Less absorption also however means less output at all temperatures. This results in a lower net output except at temperatures approaching radiative stagnation.

The lowest achievable temperature in practice is above radiation stagnation to an extent determined by the amount of nonradiative heat gain which increases approximately linearly with ($T_a - T_s$) as for the two examples in Figure 7. The relative cooling performance of the different nanocomposites at any ($T_a - T_s$) value clearly changes as the nonradiative heat input drops. It is an important issue in evaluating these nanosystems. A closer examination of this impact is thus worthwhile as it influences the preferred nanosystem, and also the choice between their spectral selectivity and broadband emission. The IR transparent cover blocks direct convective heat-exchange with outside air, but does not stop convection across the gap between the cover and the radiating plate. Conduction also occurs through the insulator at base and sides. The combined input is written as $U(T_a - T_s)$ Wm^{-2} with U the nonradiative heat gain coefficient. Practical stagnation occurs when the lines like those in Figure 7 intersect the P_{rad} plots. For $U = 2$ Wm^{-2} $°C^{-1}$ the predicted stagnation value of ($T_a - T_s$) follows in brackets for each nanoparticle doping: SiC (14 °C), SiO_2 (16.5 °C), SiC + SiO_2 (18.5 °C); and for $U = 1$ Wm^{-2} $°C^{-1}$ SiC (21 °C), SiO_2 (22.5 °C), SiC + SiO_2 (25 °C). Representative values of U were estimated to be 2 to 2.5 Wm^2 $°C^{-1}$ in low cost, simple structures like that in Figure 3 and 0.07 m^2 in area. With spectral selective coatings on aluminum an actual stagnation

DOI: 10.1021/nl903271d | *Nano Lett.* **2010,** *10,* 373-379

temperature of 17 °C below ambient was observed under our driest conditions in Sydney of about 3 mm of water vapor pressure, which is consistent with Figure 7. A surface with high broadband absorptance and near blackbody emittance $e = 0.95$ under these conditions had stagnation temperature of 12 °C below ambient, which is also consistent with our models for such a surface and those in reference.[1] Low U values are feasible and will reduce stagnation temperatures and open up the gap between spectral selective and nonspectral selective minimum temperatures. Another emerging nanotechnology, nanoporous insulation materials, and also thin vacuum insulation panels, will help. They should provide $U < 1$ Wm^{-2} $°C^{-1}$ and with additional measures to reduce convection input, $U < 0.5$ Wm^{-2} $°C^{-1}$ is possible. Then the nanocomposites will be able to pump heat in useful amounts down to 20 °C below ambient.

From Figure 7 the dual doped material will always be superior for $U \sim 2$ Wm^{-2} $°C^{-1}$. To get into the range where SiC nanoparticles by themselves are superior would require a U value under 0.3 Wm^{-2} $°C^{-1}$. In addition if we are pumping heat from a fluid then working temperatures must be several degrees above stagnation. Thus for most practical cooling applications absorbing across the sky window using both nanoparticles is preferred. Figure 7 also shows just SiO_2 nanoparticles are also very useful. A composite with SiO as in Figure 5, on a large sheet of copper bonded to small pipes, has been tested outdoors using a setup as in Figure 3 but with no air gap below the plate. Average cooling rates over a clear night when cooling a volume of already precool water by natural convection were in the range 40 to 50 Wm^2 which is consistent with Figure 7.

Amplification of net radiant output above the levels in Figure 7 is possible using heat mirror lined apertures around the emitting surface to further reduce the magnitudes of the absorbed power.[14] However the simplicity, low cost, and useful cooling performance of the systems discussed here means they are attractive for many applications. World air conditioning in 2003 needed 395 TWh of electric power per year, and by 2030 that is projected to rise to 1269 TWh.[15] Thus low cost radiative cooling technologies, alone or hybrid with existing systems, and in combination with thermally efficient structures, should be of high current interest. Future studies should explore various deployment options since reduced incidence of direct sun boosts cooling output. About 20 m^2 of these night sky radiators, could produce around 12−18 kWh of cooling per day. A boost to air conditioner performance in various hybrid modes is possible. This approach could also lead to less impact of multiple air conditioners on local microclimates in the following two ways: less power will be used and these nanoparticles will radiate much of the pumped heat into space. Other potential applications of efficient night sky cooling include water collection from the atmosphere and dehumidification, recharging of phase change coolant packs, and contributions to various refrigeration tasks such as cooling and cold storage of food and drink, select medicines and agricultural products, especially in remote, nonelectrified areas. We have set up a portable cooling system for multiple soft drink cans, using similar coatings, which works quite well. A contribution to power supply is also worth consideration. Cool can be used to enhance performance in various renewable power systems, including PV cells, solar heated thermoelectric generators, and use of various low-grade thermal sources. As an example of the latter, consider heat input to a special turbine at around 100 °C. If the turbine condenser exhausts heat at 10 °C rather than 30 °C heat-to-electric conversion efficiency rises from ∼9 to ∼12% for a 33% boost in power output.

Despite their long scientific history, few applications of surface phonon resonance in nanoparticles have emerged. Its potential for use in sky cooling is significant and low cost with the preferred elements and compounds abundant. On suitable substrates, or in suitable polymers, this study indicates these resonances could be also considered for other applications needing low cost or large areas and requiring fine spectral tuning in the IR. Filtering and narrow band IR sources are two examples.

Acknowledgment. Support for this work from an Australian Research Council Discovery Grant (ARCDP0987354) is gratefully acknowledged.

REFERENCES AND NOTES

(1) Lushiku, E. M.; Hjortsberg, A.; Granqvist, C. G. Radiative cooling with selectively infrared-emitting ammonia gas. *J. Appl. Phys.* **1982**, *53*, 5526–5530.
(2) Tazawa, M.; Kakiuchida, H.; Xu, G.; Jin, P.; Arwin, H. Optical constants of vacuum evaporated SiO film and an application. *J. Electoceram.* **2006**, *16*, 511–515.
(3) Eriksson, T. S.; Granqvist, C. G. Infrared optical properties of silicon oxynitride films: experimental data and theoretical interpretation. *J. Appl. Phys.* **1986**, *60*, 2081–2091.
(4) Högström, H.; Forsell, G.; Ribbing, C. G. Realization of selective low emittance in both thermal atmospheric windows. *Opt. Eng.* **2005**, *44*, No. 026001−1, 7.
(5) Berdahl, P. Radiative cooling with MgO and/or LiF layers. *Appl. Opt.* **1984**, *23*, 370–372.
(6) Bohren, C. F. and Huffman, D. R. *Absorption and scattering of light by small particles*; Wiley: Chichester, UK, 1998.
(7) Ribbing, C. G.; Wackelgard, E. Restrahlen bands as property indicators for materials in dielectric coatings. *Thin Solid Films* **1991**, *206*, 312–317.
(8) Henning, Th.; Mutshcke, H. Formation and spectroscopy of carbides. *Spectrochim. Acta, Part A* **2001**, *57*, 815–824.
(9) Dkakai, M.; Calcagno, L.; Makthari, A. M. Infrared spectroscopy and transmission electron microscopy of polycrystalline silicon carbide. *Mater. Sci. Semicond. Process.* **2001**, *4*, 201–204.
(10) Maxwell Garnett, J. C. Colours in metal glasses and in metallic films. *Phil. Trans. R. Soc. London, Ser. A* **1904**, *203*, 385–420.
(11) Bruggeman, D. A. G. Berechnung verschiedener physikalischer Konstanten von heterogenen Substanzen, I. Dielektrizitätskonstanten und Leitfähigkeiten der Mischkörper aus isotropen Substanzen. *Ann. Phys. Lpz.* **1935**, *24*, 636–679.
(12) *Handbook of Optical Constants of Solids*Palik, E. D., Ed; Academic: San Diego, 1998.
(13) Rothman, L. S. The HITRAN 2004 molecular spectroscopic database. *J. Quant. Spec. Rad. Trans.* **2005**, *96*, 139–2104.
(14) Smith, G. B. Amplified radiative cooling via optimised combinations of aperture geometry and spectral emittance profiles of surfaces and the atmosphere. *Sol. Energy Mater. Sol. Cells* **2009**, *93*, 1696–1701.
(15) Vattenfall A. B. *Global mapping of greenhouse gas abatement opportunities up until 2030, Building sector deep-dive*. June, 2007 see www.vattenfall.com/climate.

DOI: 10.1021/nl903271d | *Nano Lett.* **2010,** *10,* 373-379